A Molecular Signature of Gastric Metaplasia Arising in Response to Acute Parietal Cell Loss

KOJI NOZAKI,[*,‡] MASAKO OGAWA,[‡] JANICE A. WILLIAMS,[*] BONNIE J. LAFLEUR,[*] VIVIAN NG,[§] RONNY I. DRAPKIN,[§,‖] JASON C. MILLS,[¶] STEPHEN F. KONIECZNY,[#] SACHIYO NOMURA,[‡] and JAMES R. GOLDENRING[*]

[*]Nashville VA Medical Center and the Department of Surgery, Vanderbilt-Ingram Cancer Center, Vanderbilt University School of Medicine, Nashville, Tennessee; [‡]Department of Gastrointestinal Surgery, University of Tokyo, Tokyo, Japan; [§]Harvard Medical School, Dana-Farber Cancer Institute; [‖]Department of Pathology, Brigham and Women's Hospital, Harvard Medical School, Boston, Massachusetts; [¶]Department of Pathology and Immunology, Washington University School of Medicine, St. Louis, Missouri; and the [#]Department of Biological Sciences and the Purdue Cancer Center, Purdue University, West Lafayette, Indiana

Background & Aims: **Loss of gastric parietal cells is a critical precursor to gastric metaplasia and neoplasia. However, the origin of metaplasia remains obscure. Acute parietal cell loss in gastrin-deficient mice treated with DMP-777 leads to the rapid emergence of spasmolytic polypeptide/trefoil factor family 2 (TFF2)-expressing metaplasia (SPEM) from the bases of fundic glands. We now sought to characterize more definitively the pathway for emergence of SPEM.** ***Methods:*** **Emerging SPEM lineages in gastrin-deficient mice treated with DMP-777 were examined for immunolocalization of TFF2, intrinsic factor, and Mist1, and morphologically with electron microscopy. Emerging SPEM was isolated with laser-capture microdissection and RNA was analyzed using gene microarrays. Immunohistochemistry in mouse and human samples was used to confirm up-regulated transcripts.** ***Results:*** **DMP-777–induced SPEM was immunoreactive for TFF2 and the differentiated chief cell markers, Mist1 and intrinsic factor, suggesting that SPEM derived from transdifferentiation of chief cells. Microarray analysis of microdissected SPEM lineages induced by DMP-777 showed up-regulation of transcripts associated with G1/S cell-cycle transition including minichromosome maintenance deficient proteins, as well as a number of secreted factors, including human epididymis 4 (HE4). HE4, which was absent in the normal stomach, was expressed in SPEM of human and mouse and in intestinal metaplasia and gastric cancer in human beings.** ***Conclusions:*** **Although traditionally metaplasia was thought to originate from normal mucosal progenitor cells, these studies indicate that SPEM evolves through either transdifferentiation of chief cells or activation of a basal cryptic progenitor. In addition, induction of metaplasia elicits the expression of secreted factors, such as HE4, relevant to gastric preneoplasia.**

Gastric cancer remains the second leading cause of cancer-related death worldwide.[1] Although the discrete mechanisms of gastric carcinogenesis remain obscure, one constant in the etiology of gastric cancer is the loss of acid-secreting parietal cells from the fundic mucosa or oxyntic atrophy. The loss of parietal cells leads to alterations in the cells in the gastric mucosa with the emergence of metaplastic mucous cell lineages. The development of oxyntic atrophy and gastric cancer in human beings is linked strongly through a sequence of lineage changes from normal to metaplastic to neoplastic.[2] Although *Helicobacter pylori* infection is associated with the induction of atrophic gastritis and histologic progression to gastric cancer, the exact mechanisms for the development of gastric metaplasia remain obscure. In addition to their important role in luminal HCl secretion, gastric parietal cells also secrete a number of critical paracrine and autocrine regulators including sonic hedgehog[3] and the epidermal growth factor receptor ligands transforming growth factor α, amphiregulin, and heparin binding–epidermal growth factor.[4] Thus, loss of parietal cells may alter the intramucosal milieu, leading to the initiation of metaplasia. It now is clear that 2 types of mucous cell metaplasia develop in the atrophic human stomach and represent putative preneoplastic lesions: goblet cell intestinal metaplasia and spasmolytic polypeptide–expressing metaplasia (SPEM, also known as *pseudopyloric metaplasia*).[5]

In the normal gastric fundic mucosa, progenitor cells located in the gland neck give rise to 4 types of epithelial cells including pepsinogen-secreting zymogenic chief cells, acid-producing parietal cells, and 2 types of mucous cells: surface mucous cells and mucous neck cells.[6] Surface mucous cells secrete trefoil factor family 1 (TFF1) and mucin 5AC, whereas mucous neck cells secrete spasmolytic polypeptide/TFF2 and mucin 6. As mucous neck cells migrate towards the bases of fundic glands they redifferentiate into zymogenic chief cells, which secrete both pepsinogen and intrinsic factor in rodents.[6] The

Abbreviations used in this paper: HE4, human epididymis 4; MCM, minichromosome maintenance deficient; PCR, polymerase chain reaction; SPEM, spasmolytic polypeptide expressing metaplastic lineage; TACC3, transforming acidic coiled-coil–containing protein 3; TFF2, trefoil factor family 2.

0016-5085/08/$34.00
doi:10.1053/j.gastro.2007.11.058

prezymogenic cells display granules showing features intermediate between those of neck cells and zymogenic chief cells. Importantly, the transition between mucous neck cells and chief cells occurs without an intermediate transiently amplifying cell and involves the induction of the transcription factor Mist1, a specific marker for mature chief cells.[7]

Several mouse models have sought to examine influences that may lead to metaplasia. Chronic infection with *Helicobacter felis* leads to oxyntic atrophy and the emergence of SPEM, with the eventual development of dysplasia.[8,9] Oral administration of DMP-777, a cell-permeant inhibitor of neutrophil elastase, which also acts as a parietal cell–specific protonophore,[10] leads to the emergence of SPEM, but in the absence of a significant inflammatory response.[11,12] Although SPEM develops in wild-type mice after 7–10 days of DMP-777–induced parietal cell loss, SPEM develops after only a single dose in gastrin-deficient mice.[11] Importantly, emerging SPEM cells express both TFF2 and the mouse chief cell marker intrinsic factor.[11] Thus, although prevailing dogma has suggested that metaplasias arise from aberrant differentiation of normal progenitor cells, these findings suggested that metaplastic SPEM cells were derived either from a cryptic progenitor cell population at the bases of fundic glands or from transdifferentiation of chief cells expressing intrinsic factor into mucous cells expressing TFF2.

We now report that, in response to parietal cell loss, SPEM arises at the bases of gastric glands distinct from the normal progenitor cells. Loss of parietal cells leads to the observation of metaplastic cells expressing TFF2 along with the mature chief cell markers, intrinsic factor and Mist1. Microdissected emerging SPEM shows up-regulation of transcripts associated with G1/S cell-cycle transition. In addition, transcripts for a group of secreted ligands were up-regulated prominently in SPEM. In particular, the whey acidic protein domain protein human epididymis 4 (HE4) was absent from the normal stomach, but was expressed strongly in SPEM from mice, as well as in both SPEM and intestinal metaplasia in human beings. HE4 was expressed in the vast majority of intestinal-type and signet ring gastric adenocarcinomas. Our results indicate that SPEM likely develops initially from either transdifferentiation of chief cells or activation of a basal cryptic progenitor lineage. Furthermore, this metaplastic transition is associated with the up-regulation of novel secreted mediators, such as HE4, that could serve as surrogate markers of the preneoplastic process.

Materials and Methods

Gene Microarray Analysis

Gastrin-deficient mice were constructed by targeted disruption of the gastrin gene and were maintained on a C57BL/6 background.[11] Mice were treated for 1 or 3 days with oral gavage administration of DMP-777 (a gift of DuPont Pharmaceuticals), formulated in 0.5% methylcellulose (administered orally as a gavage once daily at 350 mg/kg/day). Untreated mice were used as controls. Mice were killed and their stomachs were excised and opened along the greater curvature and processed for frozen sections for laser-capture microdissection. From the untreated gastrin-deficient mice, chief cells were microdissected from the bases of gastric glands. The emerging SPEM cells were microdissected from the bases of fundic glands of DMP-777–treated gastrin-deficient mice after 1 or 3 days of oral drug administration. Cell collections (10,000 cells) and extractions of total RNA were performed as previously described.[12]

Total RNAs from microdissected cells were reverse transcribed and amplified through 2 rounds of linear amplification using a Nugen (San Carlos, CA) Ovation kit to amplify and label 10–20 ng of RNA. The resulting single-strand complementary DNA (cDNA) product was purified by binding to and elution from a Qiagen (Valencia, CA) Qiaquick column. The cDNA product then was measured and 2.2 μg of the fragmented, labeled product was hybridized to Affymetrix (Santa Clara, CA) Mouse 430 2.0 microarrays overnight, with staining and scanning performed the next day (Vanderbilt Microarray Facility). Gene expression was analyzed among microdissected cells from 4 untreated gastrin-deficient mice, 4 mice treated with DMP-777 for 1 day, and 4 mice treated with DMP-777 for 3 days. The raw gene expression data (.cel files) were converted to expression values using the Affy function in R (http://www.bioconductor.org). The expression levels between groups were compared first using an overall permutation F-test for difference between the groups (control, 1-day treatment, and 3 days of treatment) using analysis of variance; if a statistically significant overall difference was seen then pair-wise differences between control and 1 day of treatment and control and 3 days of treatment were performed using permutation *t* tests. We then reduced the candidate probe list further by requiring at least 2-fold differences between treated groups (day 1 and day 3) and control in those that showed a statistically significant pair-wise difference. All expression data analysis was performed using the SAFE package in R. Annotation and pathways were interrogated using WebGestalt software (Vanderbilt University, Nashville, TN).[13]

Quantitative Polymerase Chain Reaction

Independent of the samples collected from animals for microarray analysis, total RNA isolated from laser-capture microdissected cell collections from the stomachs of normal and DMP-777 1-day–treated and DMP-777 3-day–treated gastrin-deficient mice was analyzed by quantitative polymerase chain reaction (PCR) assays. Reverse transcription from each total RNA sample was performed using random primers and Quantiscript

Reverse transcriptase (Qiagen), for 30 minutes at 42°C. Quantitative real-time PCR was performed with a 3-step method using the Bio-Rad iCycler iQ real-time PCR detection system (Bio-Rad Laboratories, Hercules, CA). Each reaction was performed in a 50-μL mixture consisting of QuantiTect SYBR Green PCR Master Mix (Qiagen), and 1 μL of template cDNA. The sequences of the primers used are listed in supplementary Table 1 (see supplementary material online at www.gastrojournal.org). The PCR conditions for quantitative real-time PCR were as follows: 95°C for 10 minutes, 45 cycles of 94°C for 15 seconds, 60°C for 30 seconds, and 72°C for 30 seconds. Quantitation of cDNA template in each sample was determined using the comparative threshold cycle method using glyceraldehyde-3-phosphate dehydrogenase as a control, as described previously.[12] Statistical comparisons of the mean ΔΔ comparative threshold cycle between groups were determined using the Mann–Whitney *U* test.

Immunohistochemistry

Excised stomachs from gastrin-deficient mice treated with DMP-777 or untreated controls embedded in paraffin were used for immunohistochemistry analysis. Stomachs from C57BL/6 wild-type mice and sections from *H felis*–infected C57BL/6 mice (infected for 6 months, a gift from Dr Timothy C. Wang, Columbia University, New York, NY) also were examined with staining as a comparison. For immunohistochemistry, except for Mist1 staining, deparaffinized sections were pretreated with antigen retrieval using Target Retrieval solution (DakoCytomation, Glostrup, Denmark) at 120°C for 15 minutes, followed by immediate cooling using iced water. For immunohistochemistry of Mist1, Trilogy antigen retrieval solution (Cell Marque, Austin, TX) was used during the antigen retrieval procedure. Sections were treated with 2% blocking serum and then incubated with the primary antibody overnight at 4°C. Immunostaining was performed with the following primary antibodies: murine monoclonal immunoglobulin M (IgM) anti-TFF2 (a gift from Sir Nicholas Wright, Cancer Research, London, UK; 1:1000); rabbit anti-Mist1 (1:2000)[7]; murine monoclonal anti-H/K–adenosine triphosphatase (ATPase; a gift from Dr Adam J. Smolka, Medical University of South Carolina, Charleston, SC; 1:100,000); rabbit anti-HE4 (1:2000)[14]; rabbit anti-intrinsic factor (a gift from Dr David Alpers, Washington University, St Louis, MO; 1:2000); goat anti-intrinsic factor (1:2000)[7]; rabbit anti–minichromosome maintenance deficient (MCM)3 (a gift from Dr Jin Woo Kim, Catholic University of Korea, Seoul, South Korea; 1:2000); and rat monoclonal anti-Ki67 (TEC-3; DakoCytomation; 1:200).

For immunofluorescence analysis, Cy3-goat anti-mouse IgM antibody, Cy5-goat anti-mouse IgG antibody (Jackson ImmunoResearch, West Grove, PA), and Alexa488 goat anti-rabbit IgG (Invitrogen, Carlsbad, CA) were used. ProLong Gold Antifade Reagent with DAPI (Invitrogen) was used for nuclear counterstain and mounting medium.

For immunohistochemistry with detection with diaminobenzidine, the sections were incubated with biotinylated secondary antibody followed by horseradish-peroxidase–conjugated streptavidin. Chromogen was developed with diaminobenzidine (Biogenex, San Ramon, CA). For immunohistochemistry with alkaline-phosphatase detection, the sections were incubated with biotinylated secondary antibody followed by alkaline phosphatase–conjugated avidin-biotin complex. Chromogen was developed with Vector Red Substrate (Vector Laboratories, Burlingame, CA). All sections were counterstained with Gill's hematoxylin.

Sections were viewed and photographed on a Zeiss Axiophot microscope equipped with an Axiovision digital imaging system (Zeiss, Jena GmBH, Germany) or a FluoView FV1000 confocal microscope system (Olympus, Tokyo, Japan).

Two tissue arrays were used for staining of human stomach samples as previously described.[15] One tissue array contained samples of normal gastric mucosa and examples of SPEM and intestinal metaplasia from 33 gastric resections at the University of Tokyo. The second array contained normal mucosa and gastric adenocarcinomas from 44 patients resected at Vanderbilt.

Electron Microscopy Analysis

Fresh specimens from the gastric fundic region of untreated controls and 3-day DMP-777–treated gastrin-deficient mice were fixed for 2.5 hours on ice in 2.5% glutaraldehyde, 0.1 mol/L cacodylate buffer in phosphate-buffered saline. The samples were incubated overnight at 4°C in 1% osmium tetroxide (OsO_4) and 0.1 mol/L cacodylate buffer. Subsequently, the samples were subjected to an ethanol dehydration series and embedded in Spurr's resin (Ted Pella, Redding, CA). Thin sections (50–100 nm) were cut and collected on 200-mesh, formvar-coated, copper grids. After drying overnight, the grids were contrast stained with 2% depleted uranyl acetate and then stained with saturated lead citrate. Samples were examined on a Philips CM12 Electron Microscope (Eindhoven, The Netherlands).

Results

Morphologic Evidence for Transdifferentiation

Given previous results suggesting the rapid evolution of SPEM in gastrin-deficient mice,[11] we evaluated whether mature chief cells expressing the bHLH transcription factor Mist1 could give rise to SPEM in DMP-777–treated mice.[7] In untreated gastrin-deficient mice, the nuclei of mature chief cells stained with antibodies against Mist1, and mucous neck cells stained with TFF2 antibodies (Figure 1*A*). In contrast, in mice treated with

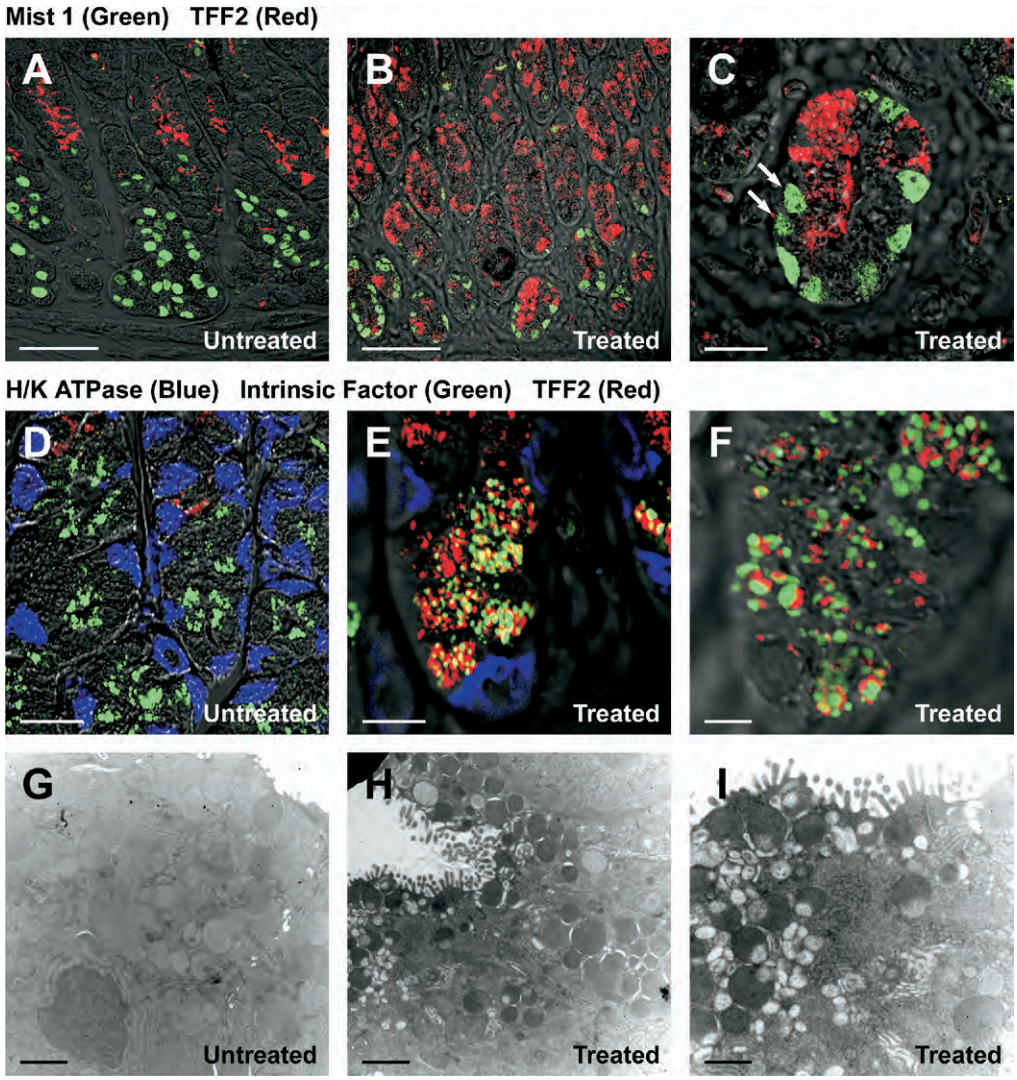

Figure 1. Characterization of emerging SPEM. (*A*) Fundic mucosa from an untreated gastrin-deficient mouse was dual immunostained for Mist1 (*green*) and TFF2 (*red*). Mist1 antibodies stained the nuclei of mature chief cells at the base of fundic glands, while TFF2 was positive in mucous neck cells in the neck region of the fundic gland. No discernible dual-staining cells were observed. *Scale bar* = 50 μm. (*B* and *C*) Mist1 and TFF2 expression in a gastrin-deficient mouse treated with DMP-777 for 3 days. The number of Mist1 immunoreactive cells (*green*) decreased in the bottom of glands, and a number of the Mist1-positive cells were dual immunoreactive for TFF2 (*red*). *Scale bar* = (*B*) 50 μm, (*C*) 10 μm. The high-power view in *C* shows the presence of cells dual labeled for Mist1 and TFF2 (*arrows*). (*D*) Mucosa from an untreated mouse stained with antibodies for H/K-ATPase (*blue*), TFF2 (*red*), and intrinsic factor (*green*). Note that there was no overlap in the staining of the 3 lineages. *Scale bar* = 20 μm. (*E* and *F*) Mucosa from a mouse treated with DMP-777 for 3 days stained with antibodies for H/K ATPase (*blue*), TFF2 (*red*), and intrinsic factor (*green*). Although parietal cells only stained with H/K-ATPase antibodies, SPEM cells at the base of the glands stained for both intrinsic factor (*green*) and TFF2 (*red*). The higher-power view in *F* shows the presence of 2 separate populations of vesicles in the SPEM cells. *Scale bar* = (*E*) 10 μm, (*F*) 4 μm. (*G–I*) Electron micrographs of chief cells from an (*G*) untreated mouse and (*H* and *I*) emerging SPEM cells from a 3-day DMP-777–treated mouse. (*G*) Chief cells showed uniformly staining zymogen granules. *Scale bar* = 2 μm. (*H* and *I*) SPEM cells at the base of fundic glands of a mouse treated with DMP-777 for 3 days contained a heterogeneous set of granule morphologies. *Scale bar* = (*G* and *H*) 2 μm, (*I*) 1 μm.

DMP-777 for 3 days, the number of Mist1 immunoreactive cells decreased at the bases of glands, and a number of the Mist1-positive cells were dual immunoreactive for TFF2 (Figure 1*B* and *C*). In the normal stomach, TFF2 and intrinsic factor were expressed in secretory granules of either mucous neck cells or chief cells, respectively (Figure 1*D*). However, in gastrin-deficient mice treated for 3 days with DMP-777, SPEM cells expressing 2 separate populations of TFF2 and intrinsic factor staining granules were present at the bases of fundic glands (Figure 1*E* and *F*). These results suggested that the loss of parietal cells in DMP-777–treated mice induced a marked alteration in the cellular phenotype of chief cells.

To examine cell lineages more precisely, the chief cells from untreated gastrin-deficient mice and emerging SPEM cells from gastrin-deficient mice treated for 3 days with DMP-777 were examined by electron microscopy (Figure 1*G–I*). In untreated animals, normal chief cells

were observed with uniformly staining zymogen granules (Figure 1*G*). However, in the DMP-777–treated cells, a heterogeneous set of granule morphologies was observed in SPEM cells at the bases of fundic glands (Figure 1*H* and *I*). The SPEM cells did contain some normal-appearing zymogen granules, generally in the perinuclear region, but they also showed large granules with electron dense material and single electron lucent circular peripheral inclusions, a morphology more consistent with mucous secretory granules. In addition, numerous smaller electron lucent granules were observed in the subluminal region. These changes in chief cell granule morphologies were observed with no morphologic evidence of apoptosis. These results indicated that chief cells were altering their granule contents to adopt morphologies more similar to mucous-secreting cells.[7]

Gene Microarray Analysis of the Emergence of SPEM

To analyze alterations in gene expression attendant with the emergence of SPEM, we used laser-capture microdissection to isolate chief cells from untreated gastrin-deficient mice as well as the emerging SPEM cells from mice treated with DMP-777 for either 1 or 3 days. Affymetrix gene microarrays were probed with the messenger RNAs (mRNAs) prepared from microdissected cells. Table 1 shows that DMP-777 treatment led to the rapid up-regulation of a number of transcripts after only 1 dose of drug. Pathway analysis showed that the most prominent sets of transcripts were involved in cell-cycle regulation and nucleotide metabolism (Table 1). In particular, 28 of the top 50 probes for up-regulated transcripts detected messages for proteins implicated in the regulation of the G1/S transition including 5 MCM proteins, ATF3, Ris2, RAD51, and ligase1. No pro-apoptotic genes were detected in the cohort of up-regulated gene transcripts in both 1 and 3 days of DMP-777 treatment (supplementary Table 2; see supplementary material online at www.gastrojournal.org). No clear pattern of gene transcript down-regulation was observed (supplementary Table 3; see supplementary material online at www.gastrojournal.org), although it is notable that there was a significant decrease in transcripts for pancreatic lipase–related protein 1, a chief cell product. In addition to the up-regulation of G1/S modulators, we also observed the prominent up-regulation of the expression for a number of secreted regulators including 2 whey acidic protein domain proteins, whey acidic protein 4-disulfide core domain 2 (HE4) and WDNM1 (Expi), interleukin-1 receptor antagonist, and epiregulin (Table 1).

Table 1. Gene Microarray Analysis of the Emergence of SPEM

Gene symbol	1 day DMP-777 vs control	3 days DMP-777 vs control
Up-regulated transcripts associated with cell cycle		
Atf3	311.4	10.1
Uhrf1	35.3	8.8
Cenph	25.7	10.7
Mcm6	25.1	36.4
Ris2[a]	21.5	41.3
Mcm5[a]	18.1	36.2
Cdca5	17.3	36.1
Mcm5[a]	13.9	18.2
Rad51	13.5	10.5
Rad51ap1[a]	12.9	6.1
Mcm10[a]	12.2	31.3
Cdc2a	11.7	7.0
Tk1	10.1	11.5
Clspn	9.5	8.5
Lig1	9.3	9.6
Cdca1	9.2	8.1
Sssca1	8.9	12.3
Dcc1	8.8	10.0
Rad51ap1[a]	8.7	7.4
Gadd45b	8.6	5.0
Rfc4	8.5	8.4
Rrm1	8.4	8.4
Rfc3	8.1	6.1
Pole	7.5	11.3
Ncapg	7.5	3.2
Prc1	7.5	6.9
Top2a	7.3	6.4
Cdca8	7.3	8.7
Ris2[a]	7.3	10.3
Prc1	7.0	7.4
Mcm10[a]	6.7	10.1
Rad54b	6.7	6.6
Up-regulated transcripts for soluble regulators		
Lgals3	46.8	153.3
Il1rn	25.4	18.5
Trip13	10.3	8.6
Fignl1	10.2	6.6
Crip1	9.5	42.6
Wfdc2	8.9	67.5
Exosc8	6.2	6.7
WDNM1	5.2	345.9
Ereg	3.6	28.9

Probes in the top 50 up-regulated transcripts detecting messages associated with the cell cycle are shown.

[a]Indicates transcripts with multiple positive probes from the Affymetrix gene microarray. Results are expressed as the fold increase in expression in samples from mice treated for either 1 or 3 days with DMP-777 compared with untreated controls. Putative secreted factors up-regulated in emerging SPEM are shown. Fold increases in expression over control are indicated. A full listing of all transcripts significantly increased greater than 2-fold is shown in supplementary Table 2 (see supplementary material online at www.gastrojournal.org).

Quantitative PCR Analysis of the Emergence of SPEM

To validate the results of the gene microarray studies, we evaluated the expression of selected up-regulated or down-regulated transcripts in microdissected lineages using quantitative PCR. We confirmed the up-regulation of G1/S-associated transcripts including MCM3, MCM5, MCM7, and ATF3 (Figure 2). We also confirmed the up-regulation of transcripts for putative soluble mediators including HE4 and inter-

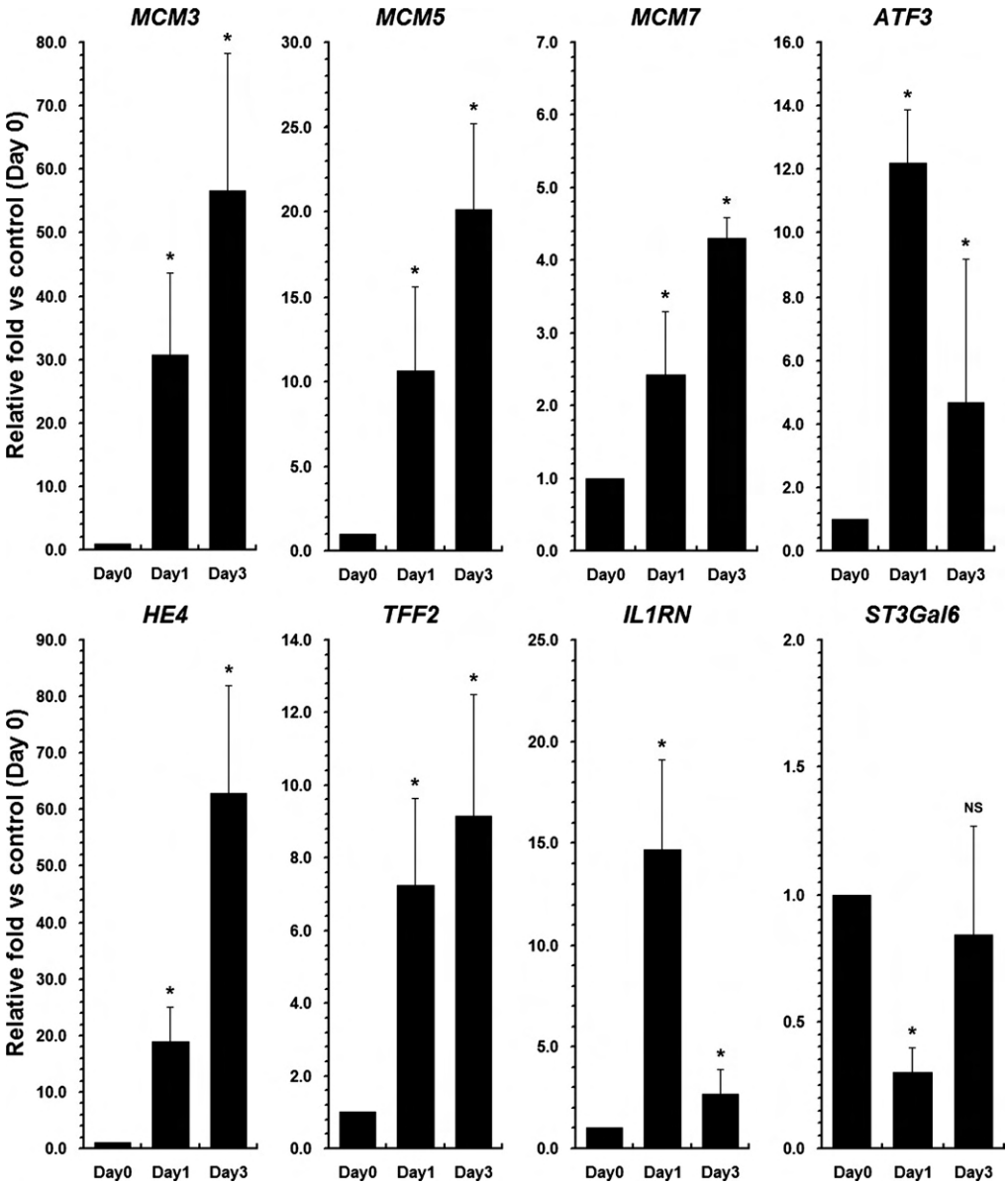

Figure 2. Quantitative PCR analysis of transcripts during the emergence of SPEM. Expression of selected up-regulated or down-regulated transcripts in microdissected lineages was examined using quantitative PCR to validate the results of the gene microarray studies. Results are represented as fold change in expression compared with levels in untreated chief cells (n = 3, ±standard error of the mean). *$P < .05$ by Mann–Whitney *U* test.

leukin-1 receptor antagonist and confirmed the down-regulation of ST3Gal6. We previously noted that Affymetrix gene arrays do not detect changes accurately in TFF2 expression.[12] However, by quantitative PCR assays, TFF2 levels were increased greater than 7-fold in emerging SPEM from DMP-777–treated animals (Figure 2). Finally, to assess the loss of differentiated chief cell markers we also evaluated transcript levels for pancreatic lipase–related proteins 1 and 2, pepsinogens A and C, and Mist1. Supplementary Figure 1*A* (see supplementary material online at www.gastrojournal.org) shows that there was a significant decrease in mRNA transcripts for all 4 protein markers. In correlation, with these findings, we also observed a rapid loss of Mist1 immunostaining at the bases of fundic gastric glands that was sustained out to 7 days of DMP-777 treatment (supplementary Figure 1*B–D*; see supplementary material online at www.gastrojournal.org).

MCM3 and Transforming Acidic Coiled-Coil–Containing Protein 3 Expression Is Increased After Acute Oxyntic Atrophy

To investigate the up-regulation of transcripts involved in G1/S transition, we examined the stomachs of DMP-777–treated or untreated gastrin-deficient mice with dual-staining with antibodies against MCM3 and Ki67, a general marker of proliferating cells (Figure 3). In untreated mice, MCM3 was localized predominantly to cells within the normal progenitor zone located in the neck region of the glands (Figure 3*A*). Nevertheless, occasionally we did observe nuclear MCM3 expression in cells at the bases of fundic glands (Figure 3*A*). In DMP-

777–treated mice, in addition to MCM3 staining in the proliferative neck region, we also observed prominent nuclear staining in SPEM cells at the bases of the fundic glands (Figure 3*B–E*). MCM3-expressing cells were distributed more widely within SPEM cells compared with Ki67-labeled cells. Although Ki67-positive cell numbers showed only a small increase after DMP-777 treatment, the number of MCM3-positive cells increased after 1 day of DMP-777 (Figure 3*B*) treatment and remained increased through 14 days of treatment (Figure 3*C–E*). The findings with Ki67 were similar to those with bromodeoxyuridine labeling (data not shown). The results suggest that MCM3 activation in emerging SPEM is more prominent than active entry into the cell cycle (Figure 3*F*).

Although these results indicated that SPEM cells emerging from the bases of gastric glands expressed MCM3, we also sought to understand the identity of MCM3-staining cells at the bases of glands in untreated mice. The observation was not specific to gastrin-deficient mice because similar MCM3-expressing cells were observed at the bases of glands in wild-type C57BL/6 mice (data not shown). We therefore performed dual staining of sections for both MCM3 and intrinsic factor, a marker of mature chief cells (Figure 4). In all cases, cells with MCM3-staining nuclei at the bases of glands also were immunoreactive for intrinsic factor, indicative of chief cells (Figure 4*F*).

We also examined the expression of transforming acidic coiled-coil–containing protein 3 (TACC3), a protein associated with the initiation of the cell cycle,[16] in DMP-777–treated mouse stomachs. Although little TACC3 expression was noted in the stomachs of untreated mice (supplementary Figure 2; see supplementary material online at www.gastrojournal.org), TACC3 expression was

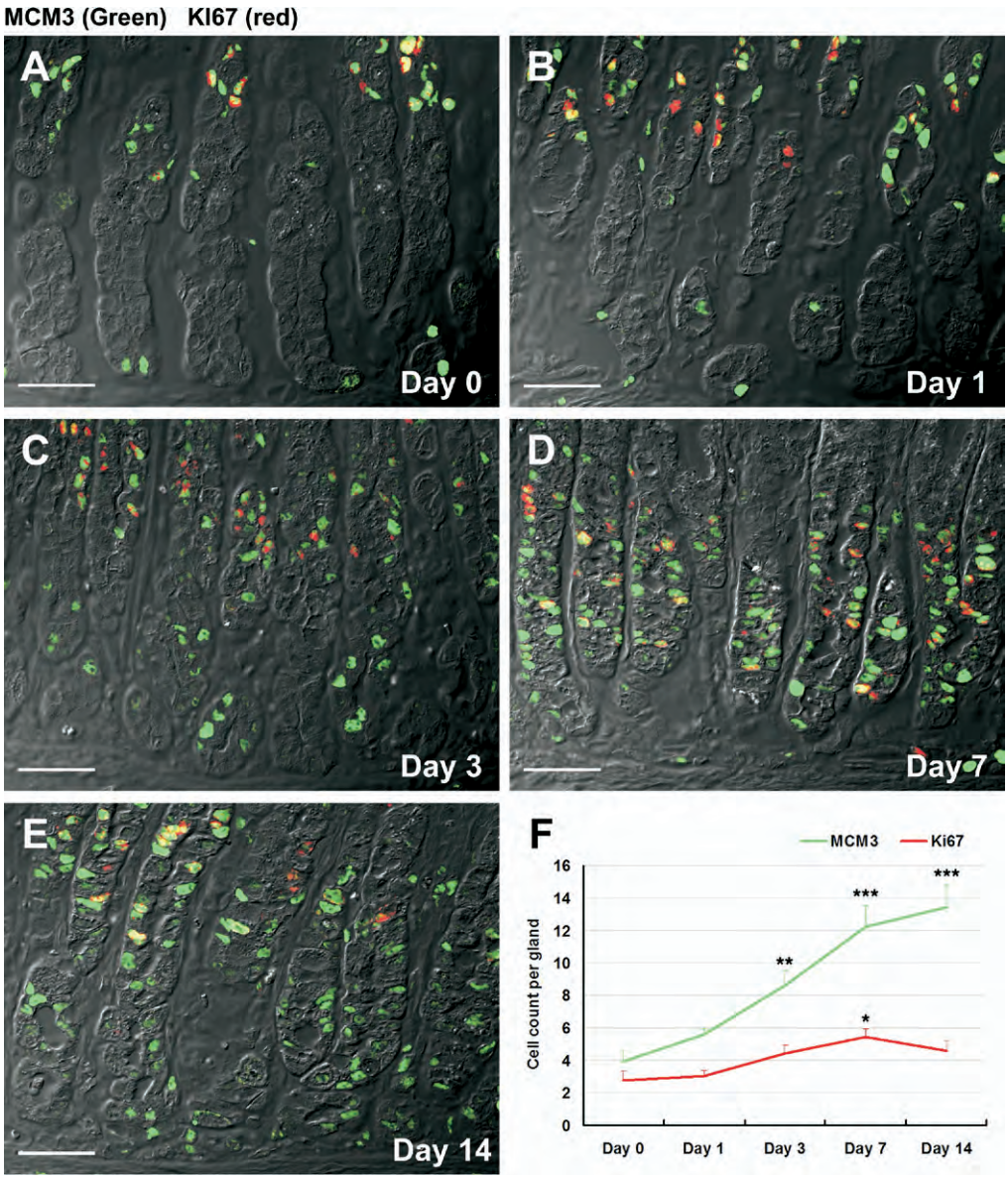

Figure 3. MCM3 expression during acute oxyntic atrophy. Sections from an (*A*) untreated mouse or mice treated with DMP-777 for (*B*) 1, (*C*) 3, (*D*) 7, or (*E*) 14 days were dual stained with antibodies against MCM3 (*green*) and antibodies against Ki67 (*red*). With increasing amounts of treatment with DMP-777, we observed an increase in MCM3 staining in cells at the bases of glands. *Scale bar* = 40 μm. (*F*) Quantification of MCM3 and Ki-67 staining showed a significant increase in MCM3 staining at days 3–14 of treatment (*green line*, $^{**}P < .01$; $^{***}P < .001$). Ki-67 staining (*red line*) showed a smaller increase, which was significant only at 7 days of treatment ($^{*}P < .05$).

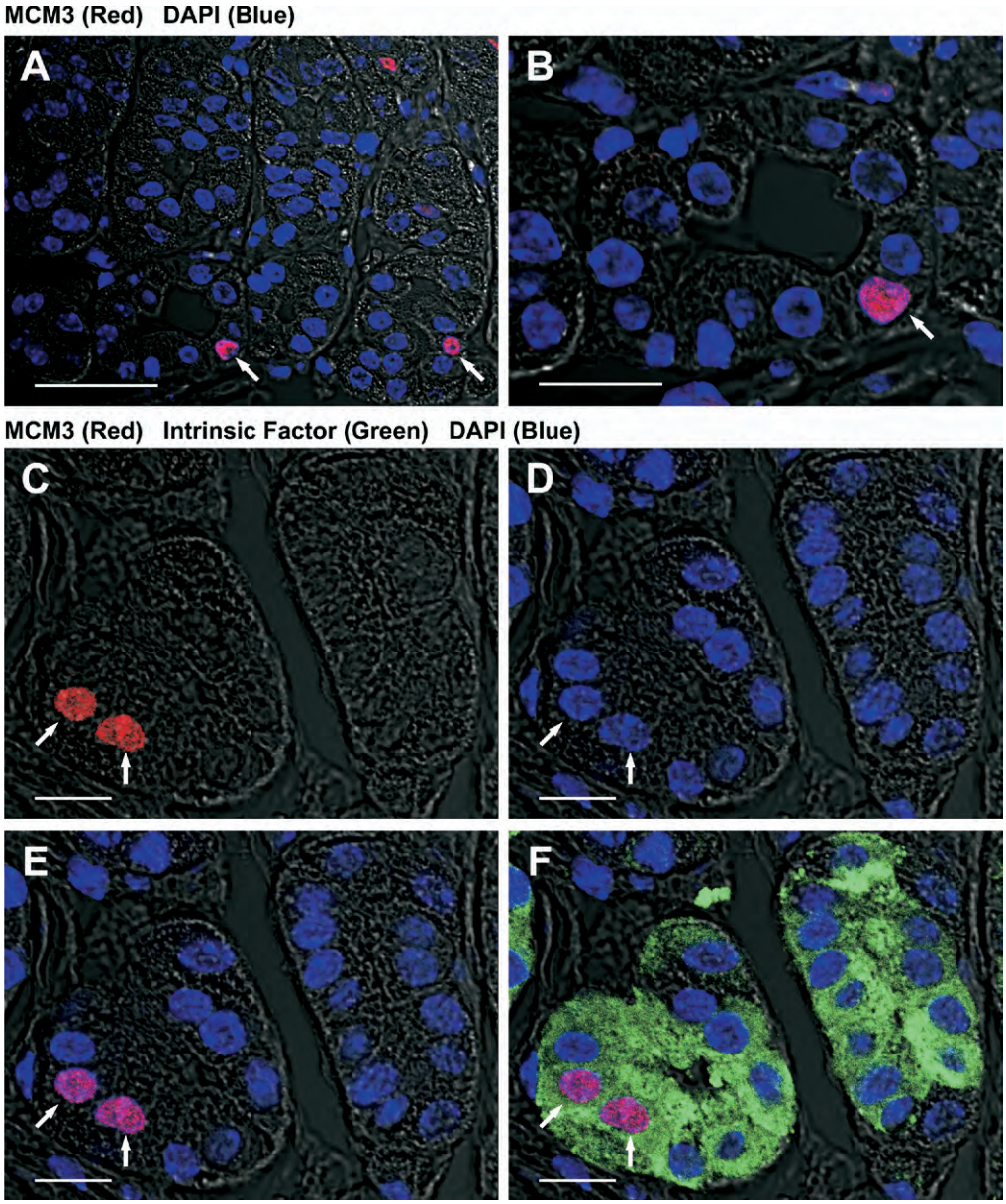

Figure 4. MCM3-positive cells at the bases of fundic glands in untreated mice are chief cells. Section from an untreated mouse stained with rabbit antibody against MCM3 (*red*), goat antibody against intrinsic factor (*green*), and DAPI (*blue*). (*A* and *B*) Nuclear MCM3 expression observed in cells at the bases of fundic glands. *Scale bar* = (*A*) 40 μm, (*B*) 20 μm. (*C* and *F*) MCM3-positive cells at the bases of fundic glands also were stained for intrinsic factor, indicating their identification as chief cells. (*C*) MCM3-positive cells (*arrows*) in the bottom of the fundic gland, (*D*) DAPI staining, (*E*) dual overlay image with MCM3 and DAPI, (*F*) triple overlay image with MCM3, intrinsic factor, and DAPI. *Arrows* indicate MCM3-positive nuclei. *Scale bar* = (*C–F*) 10 μm.

up-regulated strongly in SPEM cells at the bases of fundic glands after treatment with DMP-777 for 3 days (supplementary Figure 2; see supplementary material online at www.gastrojournal.org).

Up-Regulation of HE4 in Gastric Metaplasia and Cancer

As noted previously, the emergence of SPEM also coincided with up-regulation of several secreted factors. We therefore performed immunostaining for the whey acidic domain protein HE4 in gastrin-deficient mice. Immunostaining showed little detectable HE4 in the normal gastric mucosa of gastrin-deficient (Figure 5*A*) or wild-type C57BL/6 mice (data not shown). Nevertheless, in DMP-777–treated mice, we observed a prominent up-regulation of HE4 expression in SPEM cells at the bases of fundic glands (Figure 5*B*). In immunofluorescence studies, HE4 granules stained distinctly from TFF2 staining granules in SPEM cells (data not shown). To evaluate whether HE4 up-regulation was a common characteristic of SPEM, we also evaluated HE4 staining in the mucosa of C57BL/6 mice infected with *H felis* for 9 months. Prominent HE4 staining was observed in SPEM cells throughout the fundic mucosa in *H felis*–infected mice (Figure 5*C*).

Because the studies in mice suggested a strong association of HE4 expression with gastric metaplasia, we evaluated the expression of HE4 in the human stomach. As noted previously,[17] HE4 was not detected in the normal human fundic mucosa (Figure 5*D*). Notably, the tissue array analysis showed that HE4 was positive in all metaplastic lesions, including SPEM (Figure 5*E*), SPEM and intestinal metaplasia transitional lesions (Figure 5*F*), SPEM and intestinal metaplasia co-existing lesions (Fig-

ure 5*G* and *H*), and intestinal metaplasia (Figure 5*I*). Given the strong expression of HE4 in human gastric metaplasias, we also examined the expression of HE4 in human gastric adenocarcinoma. In contrast with TFF2, which shows a general loss in gastric cancer,[14] we observed sustained expression of HE4 in 70% of well-differentiated and moderately differentiated intestinal-type gastric adenocarcinomas (Figure 6*A–D*). Twenty percent of diffuse or poorly differentiated tumors also showed HE4 staining (Figure 6*E–F*). The HE4 staining was especially strong in 80% of signet ring adenocarcinomas (Figure 6*G–I*). Similar results were observed with immunofluorescence staining, supporting the histochemical staining results for HE4 (Figure 6*J–L*). These results indicate that HE4 is a robust biomarker for the gastric preneoplasia and the neoplastic process.

Discussion

The loss of parietal cells, oxyntic atrophy, is the most reliable correlate with gastric cancer in human beings. The results presented here suggest that the loss of parietal cells in gastrin-deficient mice leads to the rapid appearance of metaplastic cells at the bases of fundic glands expressing both mature chief cell markers and TFF2. Attendant with this process, we observed an up-regulation of genes involved in G1/S-phase transition leading to re-entry of a population of cells into the cell cycle. The metaplastic process also was associated with the up-regulation of a number of putative soluble regulators not usually present in the normal stomach mucosa. In particular, HE4 was up-regulated in gastric metaplasia in both mice and human beings and its expression was maintained in gastric adenocarcinomas. Thus, examination of the induction of gastric metaplasia in mice has revealed a number of critical regulators relevant to the preneoplastic process in human beings.

Although most views of the stomach mucosa have centered on lineage production from the normal progenitor zone in the neck of gastric fundic glands,[6] the present investigations focus attention on a potential compartment at the bases of fundic glands induced after parietal cell loss.[11] Three explanations could account for this observation (Figure 7). First, a cryptic progenitor cell population may exist at the base of fundic glands, distinct from the normal progenitor region in the neck, which would be suppressed by mucosal differentiation factors released by parietal cells. At least in gastrin-deficient mice, this explanation seems less likely because of the rapidity of metaplastic changes and the low amount of proliferation.

Second, SPEM may develop from transdifferentiation of chief cells (Figure 7). Previous studies have shown that

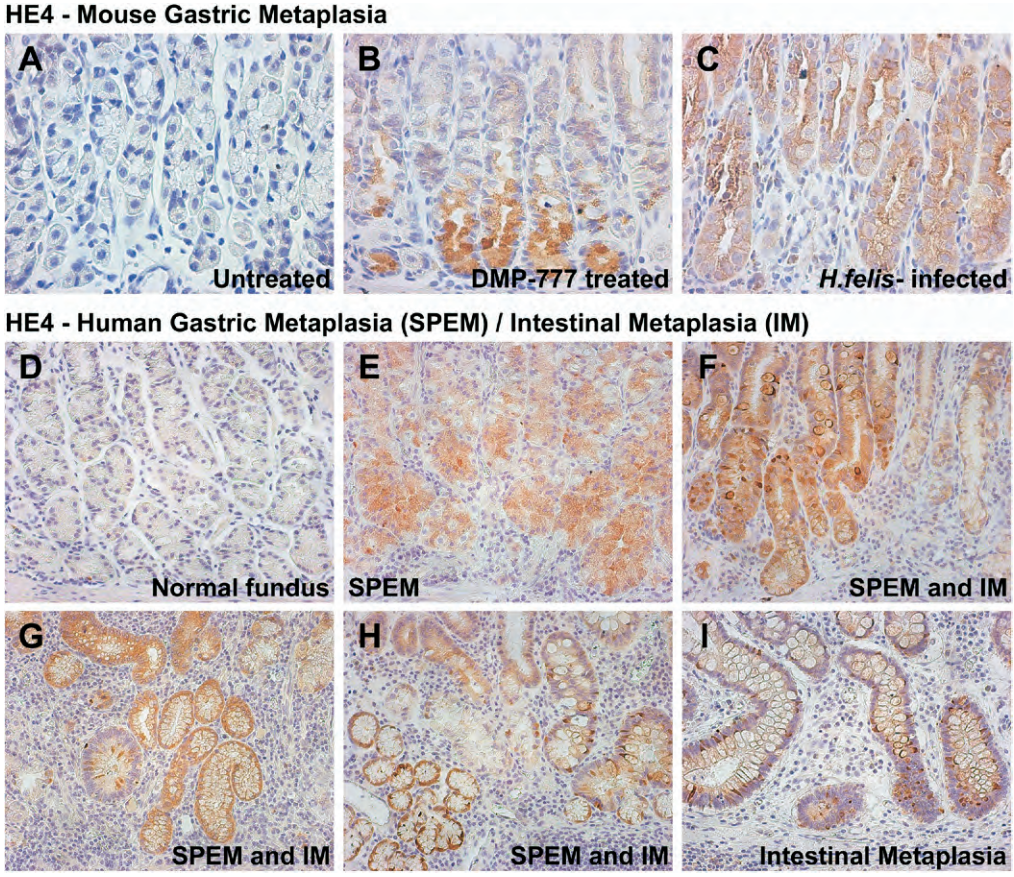

Figure 5. Up-regulation of HE4 in both SPEM and goblet cell intestinal metaplasia. We examined HE4 expression in gastric metaplasias from (*A–C*) mice and (*D–I*) human beings. (*A*) Little immunoreactivity for HE4 was detectable in the normal gastric mucosa of untreated gastrin-deficient mice. (*B*) Prominent staining for HE4 in SPEM in a gastrin-deficient mouse treated with DMP-777. (*C*) Strong staining for HE4 was observed in SPEM in the mucosa of a C57BL/6 mouse infected with *H felis* for 9 months. (*D*) No staining for HE4 was observed in the normal human gastric fundic mucosa. (*E*) SPEM from a human patient stained strongly with HE4. (*F*) SPEM and goblet cell intestinal metaplasia both stained for HE4 in a region of metaplastic transition. (*G* and *H*) In sections containing both SPEM and intestinal metaplasia, HE4 immunoreactivity was present in both metaplasias. (*I*) Intestinal metaplasia showing strong positivity for HE4.

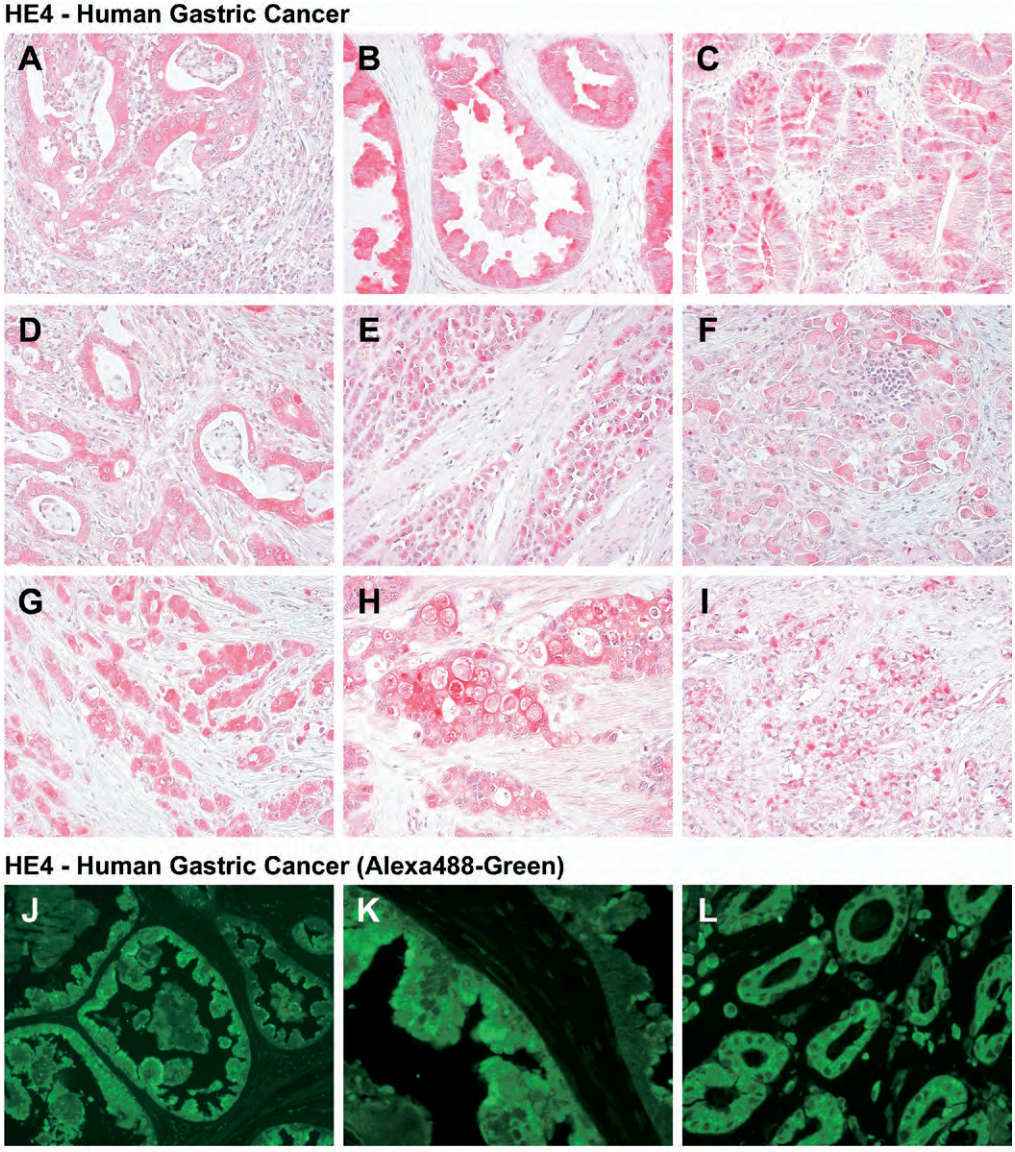

Figure 6. Immunostaining for HE4 in human gastric adenocarcinoma. (*A–I*) HE4 antibodies were used to stain sections of gastric adenocarcinomas with immunohistochemical detection with alkaline phosphatase–conjugated secondary antibody and Vector Red (Vector Laboratories, Burlingame, CA) chromogen. (*A–D*) Well-differentiated to moderately differentiated gastric cancers. Note the prominent expression of HE4 in intestinal-type gastric adenocarcinoma. (*E–G*) Poorly differentiated gastric cancers. Although the majority of poorly differentiated or diffuse cancers did not show immunoreactivity, a minority of tumors did show positivity. (*H* and *I*) Signet ring-cell–type gastric adenocarcinomas. The strongest HE4 positivity was observed in signet ring adenocarcinomas. (*J–L*) The positivity for HE4 in gastric cancers also was confirmed with immunofluorescence staining using Alexa488–anti-rabbit secondary antibodies (*green*), supporting the immunohistochemical staining results for HE4 in gastric cancers.

acute oxyntic atrophy leads to the observation of proliferating cells expressing intrinsic factor, a marker of differentiated chief cells in mice.[11] Although intrinsic factor is expressed in rare prezymogenic cells, Mist1 is expressed only in mature chief cells.[7] The observation here of Mist1-immunoreactive cells also expressing TFF2 supports chief cell transdifferentiation as the origin of SPEM. The transdifferentiation of zymogenic cells to mucous metaplasia may be a general mechanism underlying preneoplastic transition in the upper gastrointestinal tract. Means et al[18] have shown that over expression of transforming growth factor α leads to the transdifferentiation of pancreatic zymogen cells into mucous-secreting metaplastic cells. Acinar cell transdifferentiation contributes to preneoplastic PANIN lesion formation in the pancreas.[19] Likewise, loss of parietal cells may elicit the transdifferentiation of gastric zymogen-secreting chief cells. Nevertheless, these findings also may support a model compatible with both foregoing hypotheses (Figure 7). MCM3, which is required for unwinding of DNA during the G1/S transition, was expressed not only in normal progenitor cells in the gastric gland neck, but also in a small population of intrinsic factor–immunoreactive chief cells at the bases of fundic glands. Thus, a subpopulation of chief cells may have the potential for transdifferentiation, in effect, a cryptic progenitor population. Still, the rapid emergence of SPEM at the base of gastric glands in the gastrin-deficient mice after DMP-777 treatment suggests that a broader transdifferentiative process is required to account for the amount of SPEM observed after only 1 or 3 days of treatment.

Finally, it is possible that the observed lineage changes could result from arrest of chief cell lineage differentiation from mucous neck cells (Figure 7). Again, the rapidity of changes and the morphologic changes in chief cells at the bases of glands without evidence of apoptosis

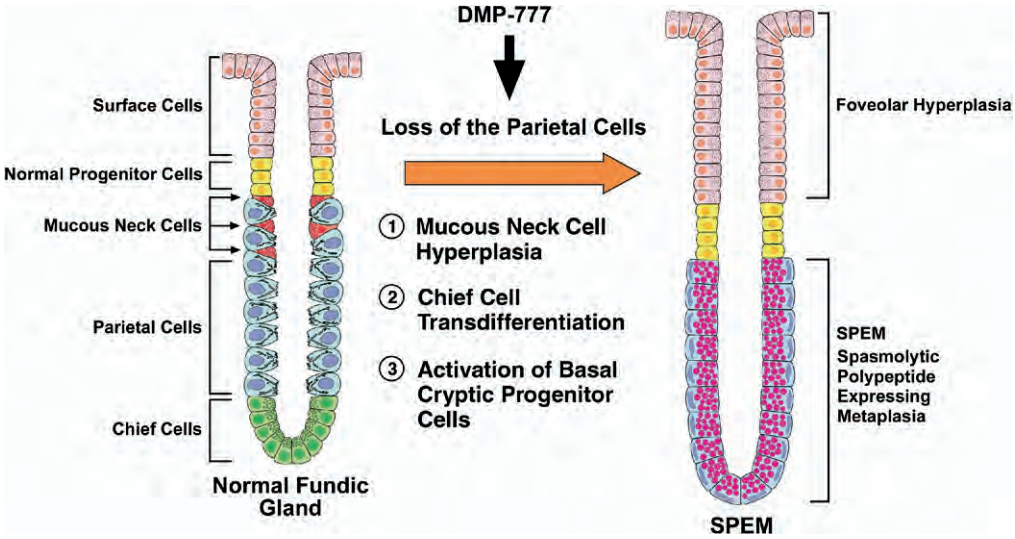

Figure 7. Hypothetical pathways for the development of SPEM from gastric fundic glands. Three hypothetical pathways for the development of SPEM arising after acute parietal cell loss: 1, mucous neck cell hyperplasia; 2, transdifferentiation of chief cells; and 3, activation of basal cryptic progenitor cells.

would seem to militate against this hypothesis. Nevertheless, it should be noted that over time with continued oxyntic atrophy, it is possible that the extent of SPEM observed may reflect in part an arrest of chief cell differentiation. We have suggested such a mechanism in studies of amphiregulin-deficient mice treated with DMP-777.[20]

The gene microarray studies of microdissected SPEM cells also support a molecular phenotype for SPEM induction. We observed the rapid up-regulation after only a single dose of DMP-777 of a cohort of gene transcripts related to the initiation of the G1/S cell-cycle transition. MCM proteins (MCM2–7) are transcribed at M/G1 and assemble into a DNA helicase responsible for unwinding chromatin before DNA synthesis.[21] MCM3 is ubiquitinated specifically in G2/M and degraded as cells exit mitosis. Still, although MCM proteins are up-regulated broadly in SPEM at the bases of fundic glands in DMP-777–treated mice, we have observed only a subset of cells entering the proliferative cycle. Thus, although some cells are re-entering the cell cycle, the observation of the up-regulation of a number of proteins involved in G1/S transition also is consistent with an alternative hypothesis. Transdifferentiation would require a major alteration in the compendium of transcripts expressed in cells without necessarily going through a proliferative cycle. Such a change in transcripts would require the unwinding of DNA, just as at the G1/S cell-cycle interface. Thus, the up-regulation of proteins involved in DNA remodeling may reflect more the process of transdifferentiation than activation of proliferation. The sustained expression of MCM3 in DMP-777–treated mice supports the concept of an alteration of the compendium of transcripts during transdifferentiation, with only limited progression through the cell cycle.

The findings presented here also suggest that acute oxyntic atrophy leads to up-regulation of gene transcripts specific for mucous cell metaplasia. The emergence of mucous cell metaplasia up-regulated specific secreted mucosal factors, including HE4, WDNM1, interleukin-1 receptor antagonist, and epiregulin. Interleukin-1 receptor antagonist has been implicated in a number of neoplastic processes.[22] Similarly, epiregulin, an epidermal growth factor receptor ligand family member with affinity for Erb4, is associated with more aggressive cancer metastasis.[23] HE4 is up-regulated early in the development of ovarian cancer and may serve as a biomarker of ovarian neoplasia.[14] Although HE4 is not expressed in the normal human gastric mucosa, we observed prominent up-regulation of HE4 expression in both intestinal metaplasia and SPEM. Importantly, HE4 expression was maintained in the vast majority of differentiated gastric adenocarcinomas. We also observed increased expression of HE4 in PANIN lesions and pancreatic adenocarcinoma (unpublished data). The current study therefore shows that factors up-regulated in the process of SPEM induction also may serve as surrogate biomarkers of gastric preneoplasia and neoplasia.

In summary, although previous views have suggested that gastric metaplasia originates from normal mucosal progenitor cells, the present results indicate that the loss of parietal cells from the gastric fundic mucosa induces alterations in the transcriptional profile of chief cells leading to changes in the cellular secretory phenotype and transdifferentiation into a mucous cell metaplasia. Attendant with these changes, particular soluble regulators such as HE4 are up-regulated in metaplasia and represent characteristic putative biomarkers for the metaplastic and preneoplastic process.

Supplementary Data

Note: To access the supplementary material accompanying this article, visit the online version of *Gas-*

troenterology at www.gastrojournal.org, and at doi: 10.1053/j.gastro.2007.11.058.

References

1. Pisani P, Bray F, Parkin DM. Estimates of the world-wide prevalence of cancer for 25 sites in the adult population. Int J Cancer 2002;97:72–81.
2. Parsonnet J, Friedman GD, Vandersteen DP, et al. *Helicobacter pylori* infection and the risk of gastric cancer. N Engl J Med 1991;325:1127–1131.
3. Stepan V, Ramamoorthy S, Nitsche H, et al. Regulation and function of the sonic hedgehog signal transduction pathway in isolated gastric parietal cells. J Biol Chem 2005;280:15700–15708.
4. Beauchamp RD, Barnard JA, McCutchen CM, et al. Localization of transforming growth factor alpha and its receptor in gastric mucosal cells. J Clin Invest 1989;84:1017–1023.
5. Schmidt PH, Lee JR, Joshi V, et al. Identification of a metaplastic cell lineage associated with human gastric adenocarcinoma. Lab Invest 1999;79:639–646.
6. Karam SM, Leblond CP. Dynamics of epithelial cells in the corpus of the mouse stomach. III. Inward migration of neck cells followed by progressive transformation into zymogenic cells. Anat Rec 1993;236:297–313.
7. Ramsey VG, Doherty JM, Chen CC, et al. The maturation of mucus-secreting gastric epithelial progenitors into digestive-enzyme secreting zymogenic cells requires Mist1. Development 2007;134:211–222.
8. Houghton J, Stoicov C, Nomura S, et al. Gastric cancer originating from bone marrow derived cells. Science 2004;306:1568–1571.
9. Wang TC, Dangler CA, Chen D, et al. Synergistic interaction between hypergastrinemia and *Helicobacter* infection in a mouse model of gastric cancer. Gastroenterology 2000;118:36–47.
10. Goldenring JR, Ray GS, Coffey RJ, et al. Reversible drug-induced oxyntic atrophy in rats. Gastroenterology 2000;118:1080–1093.
11. Nomura S, Yamaguchi H, Wang TC, et al. Alterations in gastric mucosal lineages induced by acute oxyntic atrophy in wild type and gastrin deficient mice. Am J Physiol 2004;288:G362–G375.
12. Nomura S, Baxter S, Yamaguchi T, et al. Spasmolytic polypeptide expressing metaplasia (SPEM) to pre-neoplasia in *H. felis*-infected mice. Gastroenterology 2004;127:582–594.
13. Zhang B, Kirov S, Snoddy J. WebGestalt: an integrated system for exploring gene sets in various biological contexts. Nucleic Acids Res 2005;33:W741–W748.
14. Drapkin R, von Horsten HH, Lin Y, et al. Human epididymis protein 4 (HE4) is a secreted glycoprotein that is overexpressed by serous and endometrioid ovarian carcinomas. Cancer Res 2005;65:2162–2169.
15. Leys CM, Nomura S, Rudzinski E, et al. Expression of Pdx-1 in human gastric metaplasia and gastric adenocarcinoma. Hum Pathol 2006;37:1162–1168.
16. Aitola M, Sadek CM, Gustafsson JA, et al. Aint/Tacc3 is highly expressed in proliferating mouse tissues during development, spermatogenesis, and oogenesis. J Histochem Cytochem 2003;51:455–469.
17. Bingle L, Singleton V, Bingle CD. The putative ovarian tumour marker gene HE4 (WFDC2), is expressed in normal tissues and undergoes complex alternative splicing to yield multiple protein isoforms. Oncogene 2002;21:2768–2773.
18. Means AL, Meszoely IM, Suzuki K, et al. Pancreatic epithelial plasticity mediated by acinar cell transdifferentiation and generation of nestin-positive intermediates. Development 2005;132:3767–3776.
19. Zhu L, Shi G, Schmidt CM, et al. Acinar cells contribute to the molecular heterogeneity of pancreatic intraepithelial neoplasia. Am J Pathol 2007;171:263–273.
20. Nam KT, Varro A, Coffey RJ, et al. Potentiation of oxyntic atrophy-induced gastric metaplasia in amphiregulin-deficient mice. Gastroenterology 2007;132:1804–1819.
21. Braun KA, Breeden LL. Nascent transcription of MCM2-7 is important for nuclear localization of the minichromosome maintenance complex in G1. Mol Biol Cell 2007;18:1447–1456.
22. Machado JC, Pharoah P, Sousa S, et al. Interleukin 1B and interleukin 1RN polymorphisms are associated with increased risk of gastric carcinoma. Gastroenterology 2001;121:823–829.
23. Gupta GP, Nguyen DX, Chiang AC, et al. Mediators of vascular remodelling co-opted for sequential steps in lung metastasis. Nature 2007;446:765–770.

Received August 3, 2007. Accepted November 15, 2007.

Address requests for reprints to: James R. Goldenring, MD, PhD, Department of Surgery, Epithelial Biology Program, Vanderbilt University School of Medicine, 4160A MRBIII, 465 21st Avenue South, Nashville, Tennessee 37232-2733. e-mail: jim.goldenring@vanderbilt.edu; fax: (615) 343-1591.

These studies were supported by grants from a Department of Veterans Affairs Merit Review Award, a pilot project grant from the Vanderbilt Specialized Program of Research Excellence in Gastrointestinal Cancer (1P 50 CA95103), the AGA Funderburg Award in Gastric Biology Related to Cancer, and a Discovery Grant from the Vanderbilt-Ingram Cancer Center (J.R.G.). Also supported by National Institutes of Health grant K08 DK066062 (J.C.M.) and by grant R01 DK55489 (S.F.K.). Also supported by National Institutes of Health grant K08 CA108748, the Ovarian Cancer Research Fund, the Fannie E. Rippel Foundation, and the Dunkin Donuts Rising Stars Program (R.D.). Also supported by the Jon Isenberg Award from the Foundation for Digestive Health and Nutrition/American Gastroenterological Association (K.N.).

The authors thank Drs Adam Smolka, Jin Woo Kim, Nicholas Wright, and David Alpers for the gifts of antibodies; Dr Timothy Wang for continuing discussions and sections of stomach from *Helicobacter felis*–infected mice; and Dr Joseph Roland for artistic contributions.